This paper is published as part of a PCCP Themed Issue on:

Nucleic Acid Simulations

Guest Editors: Modesto Orozco and Charles Laughton

Editorial

Nucleic Acid Simulations
Modesto Orozco and Charles Laughton, *Phys. Chem. Chem. Phys.*, 2009
DOI: 10.1039/b921472k

Perspectives

Viral assembly: a molecular modeling perspective
Stephen C. Harvey, Anton S. Petrov, Batsal Devkota and Mustafa Burak Boz, *Phys. Chem. Chem. Phys.*, 2009
DOI: 10.1039/b912884k

Simulation of DNA catenanes
Alexander Vologodskii and Valentin V. Rybenkov, *Phys. Chem. Chem. Phys.*, 2009
DOI: 10.1039/b910812b

Papers

Stabilization of radical anion states of nucleobases in DNA
Alexander A. Voityuk, *Phys. Chem. Chem. Phys.*, 2009
DOI: 10.1039/b910690a

Effects of the biological backbone on DNA–protein stacking interactions
Cassandra D. M. Churchill, Lex Navarro-Whyte, Lesley R. Rutledge and Stacey D. Wetmore, *Phys. Chem. Chem. Phys.*, 2009
DOI: 10.1039/b910747a

The impact of monovalent ion force field model in nucleic acids simulations
Agnes Noy, Ignacio Soteras, F. Javier Luque and Modesto Orozco, *Phys. Chem. Chem. Phys.*, 2009
DOI: 10.1039/b912067j

Structural ultrafast dynamics of macromolecules: diffraction of free DNA and effect of hydration
Milo M. Lin, Dmitry Shorokhov and Ahmed H. Zewail, *Phys. Chem. Chem. Phys.*, 2009
DOI: 10.1039/b910794k

Simulation of DNA double-strand dissociation and formation during replica-exchange molecular dynamics simulations
Srinivasaraghavan Kannan and Martin Zacharias, *Phys. Chem. Chem. Phys.*, 2009
DOI: 10.1039/b910792b

Sensors for DNA detection: theoretical investigation of the conformational properties of immobilized single-strand DNA
Vincenzo Barone, Ivo Cacelli, Alessandro Ferretti, Susanna Monti and Giacomo Prampolini, *Phys. Chem. Chem. Phys.*, 2009
DOI: 10.1039/b914386f

Relaxation dynamics of nucleosomal DNA
Sergei Y. Ponomarev, Vakhtang Putkaradze and Thomas C. Bishop, *Phys. Chem. Chem. Phys.*, 2009
DOI: 10.1039/b910937b

Dynamics of a fluorophore attached to superhelical DNA: FCS experiments simulated by Brownian dynamics
Tomasz Wocjan, Jan Krieger, Oleg Krichevsky and Jörg Langowski, *Phys. Chem. Chem. Phys.*, 2009
DOI: 10.1039/b911857h

A detailed binding free energy study of 2 : 1 ligand–DNA complex formation by experiment and simulation
Witcha Treesuwan, Kitiyaporn Wittayanarakul, Nahoum G. Anthony, Guillaume Huchet, Hasan Alniss, Supa Hannongbua, Abedawn I. Khalaf, Colin J. Suckling, John A. Parkinson and Simon P. Mackay, *Phys. Chem. Chem. Phys.*, 2009
DOI: 10.1039/b910574c

Molecular simulation of conformational transitions in biomolecules using a combination of structure-based potential and empirical valence bond theory
Giuseppe de Marco and Péter Várnai, *Phys. Chem. Chem. Phys.*, 2009
DOI: 10.1039/b917109f

Dependence of A-RNA simulations on the choice of the force field and salt strength
Ivana Beššeová, Michal Otyepka, Kamila Réblová and Jiří Šponer, *Phys. Chem. Chem. Phys.*, 2009
DOI: 10.1039/b911169g

Protein–DNA binding specificity: a grid-enabled computational approach applied to single and multiple protein assemblies
Krystyna Zakrzewska, Benjamin Bouvier, Alexis Michon, Christophe Blanchet and Richard Lavery, *Phys. Chem. Chem. Phys.*, 2009
DOI: 10.1039/b910888m

Evaluation of molecular modelling methods to predict the sequence-selectivity of DNA minor groove binding ligands
Hao Wang and Charles A. Laughton, *Phys. Chem. Chem. Phys.*, 2009
DOI: 10.1039/b911702d

Mesoscale simulations of two nucleosome-repeat length oligonucleosomes
Tamar Schlick and Ognjen Perišić, *Phys. Chem. Chem. Phys.*, 2009
DOI: 10.1039/b918629h

On the parameterization of rigid base and basepair models of DNA from molecular dynamics simulations
F. Lankaš, O. Gonzalez, L. M. Heffler, G. Stoll, M. Moakher and J. H. Maddocks, *Phys. Chem. Chem. Phys.*, 2009
DOI: 10.1039/b919565n

Charge transfer equilibria of aqueous single stranded DNA
Marco D'Abramo, Massimiliano Aschi and Andrea Amadei, *Phys. Chem. Chem. Phys.*, 2009
DOI: 10.1039/b915312h

Charge transfer equilibria of aqueous single stranded DNA

Marco D'Abramo,*[a] Massimiliano Aschi[b] and Andrea Amadei*[c]

Received 27th July 2009, Accepted 23rd October 2009
First published as an Advance Article on the web 28th October 2009
DOI: 10.1039/b915312h

The charge transfer thermodynamics of a simple model of DNA, a single stranded 10-mer poly-adenine oligonucleotide, in water is investigated by means of a computational/theoretical procedure, in which all the relevant environmental effects are considered. Our data indicate that water and counterions ultimately dominate the DNA reduction and oxidation free energies, which are also strongly influenced by the base position along the strand. In fact, we estimated that reduction free energies are large and negative, particularly for the bases close to the 5′ and 3′ positions, whereas the electron detachment is thermodynamically unfavoured all along the strand, but with a higher free energy cost in the central region of the molecule. Further investigation on double charging, *i.e.* one nucleobase is oxidized and one is reduced within the strand, predicts that charge-separated states are possible and thermodynamically largely stable when the ionic forms are separated by several nucleobases.

1. Introduction

Because of the DNA unique topology and ubiquitousness, charge transfer reactions in DNA molecules are involved in an uncountable number of processes relevant in biology, biochemistry, medicine[1] and nanotechnology.[2] In fact, DNA modifications, reactions leading to mutations, oxidative damage and design of nano-devices all involve charge transfer processes. Therefore, the study of DNA electronic properties has received huge interest, particularly in the last decade (for a recent review see, *e.g.*, Boussicault and Robert[3]). Despite the enormous advance of experimental methodologies able to provide a detailed picture of electron transfer in DNA,[4–9] its theoretical characterization is still challenging due to the fact that a realistic modelization must include both the electronic and the environmental effects in a coherent statistical-mechanical framework. To this end, several approaches were used to theoretically describe these processes, either approximating the solvent description as a dielectric continuum[10] or explicitly treating at atomistic level the environment interacting with the nucleobase electrons.[11–17] Beside the intrinsic differences inherent to the computational/theoretical procedure employed, all these works pointed out the dramatic effects due to the environment on DNA electronic properties and, consistently, the necessity to couple the base electronic behaviour to the environment atomic–molecular motions. Here, we apply the perturbed matrix method (PMM),[18–21] which, combining an accurate description of the nucleobase electronic properties with an efficient sampling technique, *i.e.* classical molecular dynamics simulations, is able to efficiently model the coupling between electronic states and nuclear motions. The redox thermodynamics of a (single-stranded) poly-A in solution, modelled by means of PMM, was investigated providing a quantitative estimate of nucleobase reduction/oxidation free energies and hence their dependence on sampling, base position and environment interaction. The choice of such a simple test system, *i.e.* a decamer of adenines, is motivated by the necessity of using a chemically simple, although realistic and experimentally studied, system allowing a rigorous study at an atomic level of the correlations between charge transfer along the strand and the statistical mechanics of a DNA-solvent ensemble. The results of the present study will provide the starting point for future investigations on different oligonucleotides with different sequences both single and double-stranded.

2. Theory

Similarly to the most popular quantum-mechanical/molecular-mechanics (QM/MM) approaches,[22] also in PMM it is first necessary to pre-select a portion of the simulated system to be treated at an electronic level. Such a portion, whose chemical nature and dimensions depend on the problem at hand is hereafter termed as quantum centre (QC). In the present study each base along the DNA molecule is considered as a QC embedded into the perturbing field exerted by the rest of the DNA and the solvent. Defining with $\boldsymbol{r}_n$ the nuclear coordinates of the QC, *i.e.* the coordinates of the atoms forming the QC in the simulated box and $\boldsymbol{x}$ coordinates of the atoms providing the (classical) perturbing field, we can write the QC (electronic) Hamiltonian matrix (*i.e.* the matrix expressing the Hamiltonian operator) as[18–21]

$$\begin{aligned}\tilde{H} &= \tilde{H}^0(\boldsymbol{r}_n) + \tilde{V}(\boldsymbol{r}_0, \boldsymbol{x}) \\ &\cong \tilde{H}^0(\boldsymbol{r}_n) + q_T \mathscr{V}(\boldsymbol{r}_0, \boldsymbol{x})\tilde{I} \\ &\quad + \tilde{Z}_1(\boldsymbol{E}(\boldsymbol{r}_0, \boldsymbol{x}), \boldsymbol{r}_n) + \Delta V(\boldsymbol{r}_n, \boldsymbol{x})\tilde{I}\end{aligned} \quad (1)$$

[a] *Departament de Bioquímica i Biología Molecular, Facultat de Biología, Universitat de Barcelona, Av. Diagonal 645, Barcelona 08028, Spain. E-mail: marco.dabramo@irbbarcelona.org*
[b] *Dipartimento di Chimica, Ingegneria Chimica e Materiali, Università de l'Aquila, via Vetoio (Coppito 1), 67010 l'Aquila, Italia*
[c] *Dipartimento di Scienze e Tecnologie Chimiche, Università di Roma "Tor Vergata", via della Ricerca Scientifica 1, 00133 Roma, Italia. E-mail: andrea.amadei@uniroma2.it*

where q_T is the QC total charge, $\mathscr{V}(\boldsymbol{r}_0,\boldsymbol{x})$ and $\boldsymbol{E}(\boldsymbol{r}_0,\boldsymbol{x})$ are the (perturbing) electric potential and electric field, as provided by the environment atomic charges, at a given QC $\boldsymbol{r}_0$ position (typically the mass center), $\tilde{Z}_1(\boldsymbol{E},\boldsymbol{r}_n)$ is the perturbation energy matrix explicitly given by $[\tilde{Z}_1]_{l,l'} = -\boldsymbol{E}\cdot\langle\Phi_l^0|\hat{\boldsymbol{\mu}}|\Phi_{l'}^0\rangle$ with $\hat{\boldsymbol{\mu}}$ the dipole operator and $\Delta V(\boldsymbol{r}_n,\boldsymbol{x})$ approximates all the higher order terms as a short range potential (note that the case where the quantum center is a sub-part of a molecule ΔV may also include an additive constant corresponding to a possible reference energy shift). The previous equation, providing the perturbed Hamiltonian matrix $\tilde{H}$ for a quantum center interacting with a semi-classical atomic-molecular environment, may be equivalently expressed in the typical operator notation

$$\begin{aligned}\hat{H} &= \hat{H}^0 + \hat{V}\\ &\cong \hat{H}^0 + q_T\mathscr{V} - \boldsymbol{E}\cdot\hat{\boldsymbol{\mu}} + \Delta V\end{aligned} \tag{2}$$

with the perturbation operator $\hat{V}$ physically corresponding to the perturbation due to the ground state environment atomic-molecular field acting on the QC. The eigenvectors of $\tilde{H}$, *i.e.* the eigenstates of $\hat{H}$, can be used to obtain the perturbed QC electronic properties for each QC perturbed state at each atomic configuration as provided by any sampling method, *e.g.* molecular dynamics (MD) simulations. The above theoretical framework provides an excellent description of quantum processes within complex molecular systems when the perturbing electric field is approximately homogeneous over the size of the selected QC and, of course, the definition of the QC is appropriate, *i.e.* all the quantum processes of interest may be defined *via* QC degrees of freedom and hence the perturbing atomic environment may be properly treated as a a semi-classical system. In this way PMM combined with MD simulations may furnish a very efficient theoretical–computational procedure still providing a high-level description of the quantum properties while allowing an extended sampling of the system phase-space. In this case the quantum processes we consider, require a spatially rather extended QC the above approximations and may result in a less accurate description of the perturbation operator, moreover forcing the use of a lower level of unperturbed electronic treatment.

We may combine PMM calculations, providing the perturbed electronic energies and properties, with statistical mechanical derivations in order to obtain the free energy variation due to QC state transitions.[19,20,23–27] For a charge transfer reaction, the case of interest in the present paper and previously investigated for simpler systems,[28–31] we may express the free energy change due to charging the QC as

$$\Delta A = -k_B T \ln\langle e^{-\beta\Delta\mathscr{W}'}\rangle \cong -k_B T \ln\langle e^{-\beta\Delta(\varepsilon'+q_T\mathscr{V})}\rangle \tag{3}$$

where $\Delta\mathscr{W}'$ is the energy variation of the whole system due to QC charging, $\Delta(\varepsilon'+q_T\mathscr{V})$ the corresponding change of QC perturbed ground state energy when disregarding the quantum vibrational energy and short range potential[20,27] (ε' is the ground state eigenvalue of $\tilde{H}^0 + \tilde{Z}_1$) and the average is typically taken in the uncharged QC ensemble. Note that for a charging process no relevant change of the vibrational partition function and atomic short range potential is expected and in usual MD atomistic force-field no atomic polarization beyond the pair additive dispersion interaction is considered and hence the environment internal energy is unchanged for any QC state transition. For a single stranded DNA molecule made of n bases we may therefore express the free energy change for the lth base charging $B_l \rightarrow B_l^{\pm}$, $l = 1,n$ *via*

$$\begin{aligned}\Delta A_{B_l\rightarrow B_l^{\pm}} &= -k_B T \ln\langle e^{-\beta\Delta\mathscr{W}'_{B_l\rightarrow B_l^{\pm}}}\rangle_{B_l}\\ &\cong -k_B T \ln\langle e^{-\beta\Delta(\varepsilon'+q_T\mathscr{V})_{B_l\rightarrow B_l^{\pm}}}\rangle_{B_l}\end{aligned} \tag{4}$$

which may be easily extended to multiple charging processes *via* the use of multiple energy variations, providing for the double charging B_l, $B_{l'} \rightarrow B_l^{\pm}$, $B_{l'}^{\pm}$, $l \neq l'$

$$\begin{aligned}\Delta A_{B_l,B_{l'}\rightarrow B_l^{\pm},B_l^{\pm}} &= -k_B T \ln\langle e^{-\beta\Delta\mathscr{W}'_{B_l,B_{l'}\rightarrow B_l^{\pm},B_{l'}^{\pm}}}\rangle_{B_l,B_{l'}}\\ &= -k_B T \ln\langle e^{-\beta\Delta\mathscr{W}'_{B_l,B_{l'}\rightarrow B_l^{\pm},B_{l'}}} e^{-\beta\Delta\mathscr{W}'_{B_l^{\pm},B_{l'}\rightarrow B_l^{\pm},B_{l'}^{\pm}}}\rangle_{B_l,B_{l'}}\\ &\cong -k_B T \ln\langle e^{-\beta\Delta(\varepsilon'+q_T\mathscr{V})_{B_l,B_{l'}\rightarrow B_l^{\pm},B_{l'}}}\\ &\quad\times e^{-\beta\Delta(\varepsilon'+q_T\mathscr{V})_{B_l^{\pm},B_{l'}\rightarrow B_l^{\pm},B_{l'}^{\pm}}}\rangle_{B_l,B_{l'}}\end{aligned} \tag{5}$$

It is important to remark that the QC definition we use (*i.e.* for each charge-transfer process a single base embedded in the perturbation of all the rest) implies that we disregard any excitonic effect and consider only physical states where the excess charge is localized in a unique base of the DNA molecule. Inclusion of higher order effects, although in principle possible within the PMM framework by using a more complex QC, *e.g.* two neighbouring bases, is beyond the scope of the present paper.

3. Computational methods

For the unperturbed states of the nucleobases we utilized B3LYP functional in the context of the density functional theory in conjunction with 6-311++G(d,p) atomic basis set. Unperturbed electronic properties for the first nine excited states were calculated by means of the time-dependent density functional theory (TD-DFT) as implemented in the Gaussian software.[32] Single strand poly-A formed by ten nucleobases was simulated for 100 ns at 300 K using the isokinetic temperature coupling,[33] the coordinates were saved every 2 ps and the time step was 2 fs. Molecular dynamics simulations in the NVT ensemble were performed using the Gromacs software package;[34] vibrational motions were removed by applying the LINCS algorithm and long-range electrostatics was calculated *via* the particle mesh Ewald procedure.[35] The initial configuration was extracted from standard B-DNA geometry, built by means of X3DNA[36] software. PARMBSC0[37] force field for DNA and the SPC model[38] for water were used. Error bars of the free energy profiles were estimated by a statistical block procedure.

4. Results and discussion

4.1 Redox free energies

The energies of the anionic and cationic forms of the isolated adenine, as obtained by our calculations, were compared with experimental and theoretical data available in the literature, Table 1. Beside small differences, it is clear that isolated (gas-phase) adenine may be hardly oxidized (ionization energy of 782 kJ mol^{-1}) and its electron affinity is positive (44 kJ mol^{-1}). When adenine is involved in a solvated single strand such a behaviour is strongly modified as shown in Fig. 1. The reduction free energies calculated for the adenine bases along the solvated strand are all largely negative (Fig. 1, bottom panel), particularly at 5′ and 3′ terminal ends where we estimated values of about −800 and −1100 kJ mol^{-1}, respectively. Similarly, the adenine oxidation free energies along the solvated strand (Fig. 1, upper panel), although still positive, are all dramatically reduced with respect to the unperturbed (gas-phase) oxidation energy, in particular at both terminal ends. Such a remarkable effect of the perturbing field embedding each adenine in the strand, clearly shows that the perturbation due to the DNA negatively charged phosphate groups, destabilizing/stabilizing the adenine anionic/cationic form, is overcompensated by the solvent effect (note that phosphate groups perturbation provides unstable, *i.e.* positive, reduction free energies and optimal, *i.e.* lowest, oxidation free energies in the middle of the strand). Interestingly, the redox free energies of the central bases are virtually identical within the noise, suggesting that in longer oligomers a large amount of adenines might have the same redox behaviour. Finally, the mean charging energies and relative standard deviations (Table 2) point out that large fluctuations of the charging energy occur and hence a proper sampling of the low energy configurations, severely affecting the free energy values, is essential for a proper estimate of the redox thermodynamics.

Table 1 Ionization energies and electron affinities for isolated (gas-phase) adenine

	This work	Other works (theor.)	Exp.
Ionization energies/kJ mol^{-1}	782	772 to 785[a]	797 to 825[a]
Electron affinities/kJ mol^{-1}	44	33 to 151[b]	43 to 54[b]

[a] Taken from the work of Russo *et al.*[39] and references therein. [b] Taken from the work of Roca-Sanjuán *et al.*[40] and references therein.

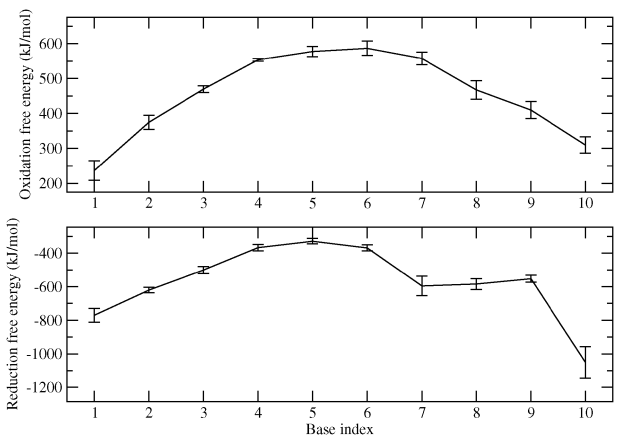

Fig. 1 Adenine oxidation (upper panel) and reduction free energies (bottom panel).

Table 2 Ensemble averages and fluctuations of the charging energies as obtained by our PMM/MD procedure

	Base 1		Base 5	
	Average	Std. dev.	Average	Std. dev.
$\Delta\mathscr{U}'_{B_l\to B_l^+}$ (kJ mol^{-1})	842	133	803	51
$\Delta\mathscr{U}'_{B_l\to B_l^-}$ (kJ mol^{-1})	−77	146	−21	61

4.2 Charge-separated states

In order to address the issue of the thermodynamic stability of charge-separated states, we considered the free energy profiles for double charging of the strand with the cationic or anionic adenine form in the corresponding most stable position (5′ or 3′ terminal end, respectively) and locating the opposite ionic form along the remaining nucleobases. Such double charging states mimic the experimental charge-separated states as provided by injecting a charge into the strand *via* a redox reaction at one of the terminal ends. In Fig. 2 we show the double charging free energy profiles for both the anionic 3′ terminal end (solid line) and cationic 5′ terminal end (dashed line) conditions. The figure clearly indicates the presence of several largely stable charge-separated states, with the state defined by the adenine ionic forms just at the terminal ends corresponding to the free energy minimum. Interestingly, for both free energy profiles, the charge separation occurring at adjacent or close bases is relatively unstable, with the curve corresponding to the cationic 5′ terminal end providing largely unstable free energies if less than five nucleobases between the ionic adenines are present. Such remarkable results revealing a huge thermodynamic tendency of the solvated poly-A to form

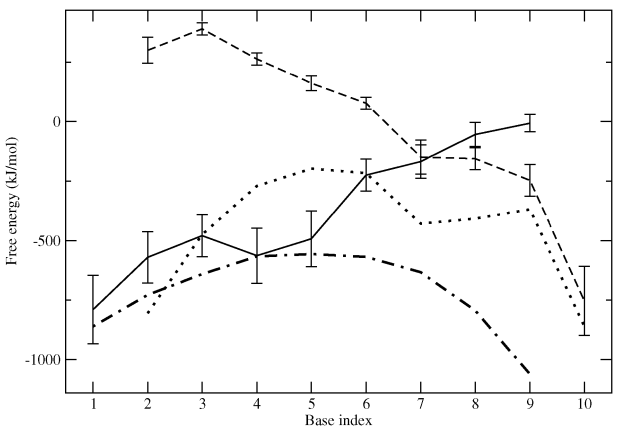

Fig. 2 Double charging free energy profiles for the 3′ anionic terminal end (solid line) and for the 5′ cationic terminal end (dashed line). Double charging free energy profiles assuming independent charging energies are also shown for cationic 5′ terminal end (dotted line) and for 3′ anionic terminal end (dashed-dotted line).

charge-separated states and showing that the direct interaction between the charged bases is overcompensated by environmental effects, also indicate that an injection of a positive or a negative charge into the DNA strand may result in rather different charge transfer behaviour. In Fig. 2 we also show the double charging free energy profiles for cationic 5′ terminal end (dotted line) and anionic 3′ terminal end (dashed-dotted line) as obtained by assuming independent charging energies, *i.e.* by using the proper sum of the free energy values in Fig. 1, including only an electrostatic constant term given by the simple charge–charge interaction evaluated at the mean distance of the ionic adenines. From the figure it is evident that neglecting the coupling between the charging processes results in completely wrong free energy estimates except when several nucleobases separate the ionic forms, thus showing the large correlation of the charging energies due to the environment perturbation field.

In order to dissect the environment perturbation into the intramolecular and solvent (including the counterions) effects, we recalculated the double charging free energy profile for the anion 3′ terminal end when considering either the perturbation field due only to the intramolecular environment or due only to the solvent environment, as shown in Fig. 3. From the figure it is evident that the two free energy profiles present opposite trends with the solvent stabilizing charge separated states at increasing distances of the charged bases. Interestingly, a comparison with the double charging free energy profile obtained by considering the whole perturbation field (already shown in Fig. 2 and also reported in Fig. 3) clearly indicates that the solvent perturbation overcompensates the intramolecular effect.

Finally, to study the effect of DNA conformational fluctuations on the charge separation process we have considered the correlation map between the end-to-end distance, as obtained by the MD trajectory and providing a relevant conformational coordinate, and the double charging energy as obtained by PMM calculations along the same MD trajectory. Such a correlation map for the 3′ anionic terminal end condition with the positive charge located on the basis 1, 5 and 9 shown in Fig. 4, reveals a weak correlation resulting in a reduced low energy tail for the compact conformation basin

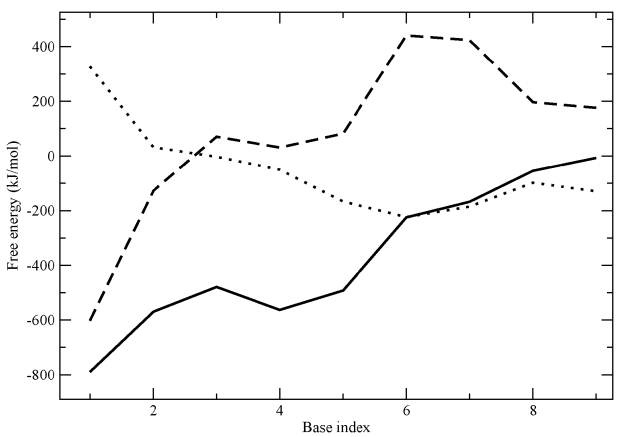

Fig. 3 Double charging free energy profiles considering solvent (dashed line), intramolecular (dotted line) and both (solid line) effects.

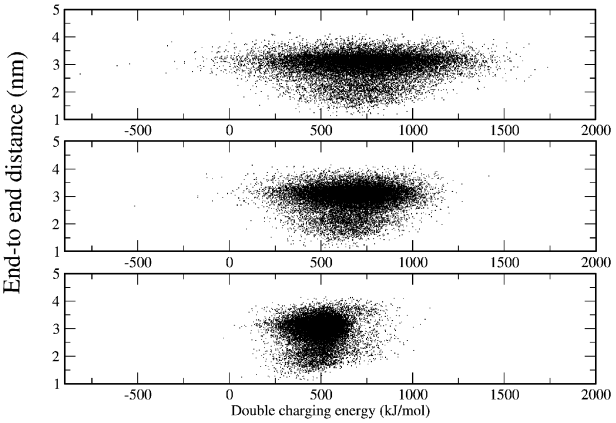

Fig. 4 Correlation map between the end-to-end distance and the double charging energy corresponding to the 3′ anionic terminal end condition with the positive charge located on the basis 1 (upper panel), 5 (middle panel) and 9 (bottom panel).

(centered at about 2 nm). Interestingly, within the extended conformation basin (by far the main conformational region, centered at about 3 nm) the double charging energy and end-to-end distance fluctuations are essentially uncorrelated, with a rather extended low energy tail determining the double charging free energy. Such results indicate that the double charging process, in particular for the charge separated state where the two terminal ends are involved, largely stabilizes the extended conformation.

5. Conclusions

In this work we characterized by means of PMM and MD simulations the redox behaviour of a single stranded poly-A in solution. The results clearly indicate the dramatic solvent effect largely determining the redox free energy profile along the strand. Moreover, the evaluation of the free energies of charge-separated states, as defined by double charging processes, reveals the intrinsic tendency of solvated poly-A to form charge-separated states, with the corresponding thermodynamic stability favoured by the increase of the distance between the charged bases clearly showing that charge–charge interaction is largely overcompensated by the environment perturbation effect. Our data also indicate that an injection of a positive or a negative charge into the DNA strand may result in rather different charge transfer behaviour, hence suggesting a different kinetic mechanism for positive and negative charge transfer reactions in DNA. Such remarkable results, in line with experimental data[6,7] demonstrating the existence of long-lived charge-separated states, point out the complexity of charge transfer equilibria in DNA, where the subtle balance between the intramolecular and solvent perturbation fields makes DNA molecules in solution particularly suited for a large variety of redox processes.

References

1 S. Steenken, *Chem. Rev.*, 1989, **89**, 503–520.
2 D. Porath, G. Cuniberti and R. D. Felice, *Top. Curr. Chem.*, 2004, **237**, 183–227.
3 F. Boussicault and M. Robert, *Chem. Rev.*, 2008, **108**, 2622–2645.

4 S. O. Kelley and J. K. Barton, *Science*, 1999, **283**, 375–381.
5 M. A. O'Neill and J. K. Barton, *Charge Transfer in DNA: from Mechanism to Applications*, Wiley, New York, 2005.
6 T. Takada, K. Kawai, X. Cai, A. Sugimoto, M. Fujitsuka and T. Majima, *J. Am. Chem. Soc.*, 2004, **126**, 1125–1129.
7 T. Takada, K. Kawai, M. Fujitsuka and T. Majima, *J. Am. Chem. Soc.*, 2006, **128**, 11012–11013.
8 K. Kawai, Y. Osakada, M. Fujitsuka and T. Majima, *Chem.–Eur. J.*, 2008, **14**, 3721–3726.
9 F. D. Lewis, H. Zhu, P. Daublain, K. Sigmund, T. Fiebig, M. Raytchev, Q. Wang and V. Shafirovich, *Photochem. Photobiol. Sci.*, 2008, **7**, 534–539.
10 J. Gu, Y. Xie and H. F. Schaefer, *Nucleic Acids Res.*, 2007, **35**, 5165–5172.
11 Y. A. Mantz, F. L. Gervasio, T. Laino and M. Parrinello, *Phys. Rev. Lett.*, 2007, **99**, 058104.
12 M. D. Peraro, P. Ruggerone, S. Raugei, F. L. Gervasio and P. Carloni, *Curr. Opin. Struct. Biol.*, 2007, **17**, 149–156.
13 T. Steinbrecher, T. Koslowski and D. A. Case, *J. Phys. Chem. B*, 2008, **112**, 16935–16944.
14 T. Kubar, P. B. Woiczikowski, G. Cuniberti and M. Elstner, *J. Phys. Chem. B*, 2008, **112**, 7937–7947.
15 T. Kubar and M. Elstner, *J. Phys. Chem. B*, 2008, **112**, 8788–8798.
16 N. R. A. A. Voityuk and K. Siriwong, *Angew. Chem., Int. Ed.*, 2004, **43**, 624–627.
17 A. Bongiorno, *J. Phys. Chem. B*, 2008, **112**, 13945–13950.
18 R. Spezia, M. Aschi, A. Di Nola and A. Amadei, *Chem. Phys. Lett.*, 2002, **365**, 450–456.
19 A. Amadei, M. D'Abramo, C. Zazza and M. Aschi, *Chem. Phys. Lett.*, 2003, **381**, 187–193.
20 A. Amadei, M. D'Alessandro and M. Aschi, *J. Phys. Chem. B*, 2004, **108**, 16250–16254.
21 A. Amadei, F. Marinelli, M. D'Abramo, M. D'Alessandro, M. Anselmi, A. Di Nola and M. Aschi, *J. Chem. Phys.*, 2005, **122**, 124506.
22 W. T. H. M. Senn, *Angew. Chem., Int. Ed.*, 2009, **48**, 1198–1229.
23 M. D'Alessandro, F. Marinelli, M. D'Abramo, M. Aschi, A. Di Nola and A. Amadei, *J. Chem. Phys.*, 2005, **122**, 124507.
24 M. D'Alessandro, M. Aschi, M. Paci, A. Di Nola and A. Amadei, *J. Phys. Chem. B*, 2004, **108**, 16255–16260.
25 M. Aschi, M. D'Abramo, F. Ramondo, I. Daidone, M. D'Alessandro, A. Di Nola and A. Amadei, *J. Phys. Org. Chem.*, 2006, **19**, 518–530.
26 A. Amadei, M. D'Abramo, I. Daidone, M. D'Alessandro, A. Di Nola and M. Aschi, *Theor. Chem. Acc.*, 2007, **117**, 637–647.
27 A. Amadei, M. Aschi and A. D. Nola, in *Solvation effects. Methods and Applications*, Springer series: *Challenges and Advances in Computational Chemistry and Physics*, Springer-Verlag, Berlin.
28 M. Aschi, C. D. Teodoro, A. Amadei, D. Roccatano, F. Malatesta and L. Ottaviano, *ChemPhysChem*, 2005, **6**, 53–689.
29 M. Aschi, M. D'Alessandro, M. Pellegrino, A. D. Nola, M. D'Abramo and A. Amadei, *Theor. Chem. Acc.*, 2008, **119**, 469–476.
30 C. Zazza, A. Amadei, A. Palma, N. Sanna, S. Tatoli and M. Aschi, *J. Phys. Chem. B*, 2008, **112**, 3184–3192.
31 C. Zazza, A. Amadei, N. Sanna and M. Aschi, *Chem. Commun.*, 2008, 3399–3401.
32 M. J. Frisch, G. W. Trucks, H. B. Schlegel, G. E. Scuseria, M. A. Robb, J. R. Cheeseman, J. A. Montgomery, Jr., T. Vreven, K. N. Kudin, J. C. Burant, J. M. Millam, S. S. Iyengar, J. Tomasi, V. Barone, B. Mennucci, M. Cossi, G. Scalmani, N. Rega, G. A. Petersson, H. Nakatsuji, M. Hada, M. Ehara, K. Toyota, R. Fukuda, J. Hasegawa, M. Ishida, T. Nakajima, Y. Honda, O. Kitao, H. Nakai, M. Klene, X. Li, J. E. Knox, H. P. Hratchian, J. B. Cross, V. Bakken, C. Adamo, J. Jaramillo, R. Gomperts, R. E. Stratmann, O. Yazyev, A. J. Austin, R. Cammi, C. Pomelli, J. Ochterski, P. Y. Ayala, K. Morokuma, G. A. Voth, P. Salvador, J. J. Dannenberg, V. G. Zakrzewski, S. Dapprich, A. D. Daniels, M. C. Strain, O. Farkas, D. K. Malick, A. D. Rabuck, K. Raghavachari, J. B. Foresman, J. V. Ortiz, Q. Cui, A. G. Baboul, S. Clifford, J. Cioslowski, B. B. Stefanov, G. Liu, A. Liashenko, P. Piskorz, I. Komaromi, R. L. Martin, D. J. Fox, T. Keith, M. A. Al-Laham, C. Y. Peng, A. Nanayakkara, M. Challacombe, P. M. W. Gill, B. G. Johnson, W. Chen, M. W. Wong, C. Gonzalez and J. A. Pople, *GAUSSIAN 03 (Revision C.02)*, Gaussian, Inc., Wallingford, CT, 2004.
33 D. J. Evans and P. T. Cummings, *Mol. Phys.*, 1991, **72**, 893.
34 D. van der Spoel, R. van Drunen and H. J. C. Berendsen, *Groningen Machine for Chemical Simulations*, Department of Biophysical Chemistry, BIOSON Research Institute, Nijenborgh 4 NL-9717, AG Groningen, 1994.
35 T. A. Darden, D. M. York and L. G. Pedersen, *J. Chem. Phys.*, 1993, **98**, 10089.
36 X.-J. Lu and W. K. Olson, *Nucleic Acids Res.*, 2003, **31**, 5108–5121.
37 A. Pérez, I. Marchán, D. Svozil, J. Sponer, T. E. Cheatham, C. A. Laughton and M. Orozco, *Biophys. J.*, 2007, **92**, 3817–3829.
38 H. J. C. Berendsen, J. P. M. Postma, W. F. van Gunsteren and J. Hermans, *Intermolecular Forces*, ed. B. Pullmann, D. Reidel Publishing Company, Dordrecht, 1981, pp. 331–342.
39 N. Russo, M. Toscano and A. Grand, *J. Comput. Chem.*, 2000, **21**, 1243–1250.
40 D. Roca-Sanjuán, M. Merchán, L. Serrano-Andrés and M. Rubio, *J. Chem. Phys.*, 2008, **129**, 095104.

